Enhancing the efficiency of the gallium indium nitride (InGaN) solar cell by optimizing the effective parameters

A. Bouadi[a], H. Naim[a,b*], A. Djelloul[c], Y. Benkrima[d], R. Fares[e]
[a]*Laboratory for Analysis and Applications of Radiation (LAAR), Department of Physics, University of Science and Technology of Oran (USTO)*
[b]*Laboratory of Thin Films Physics and Materials for Electronics (LPCMME); University Of Oran1, 31000 Oran, Algeria*
[c]*Centre de Recherche en Technologie des Semi-Conducteurs pour l'Energétique 'CRTSE' 02 Bd Frantz Fanon. BP 140. 7 Merveilles. Alger. Algérie*
[d]*Ecole normale supérieure de Ouargla, 30000 Ouargla*
[e]*LGIDD, Faculty of SESNV, University of Relizane, Algeria*

The present work aims to improve the power and the conversion efficiency of solar cells, using the PC1D simulator, to study the performances of the solar cells based on (InGaN). The paper focuses first on optimization of the technological and geometrical parameters such as doping and the thickness of the layers to investigate their influence on the conversion efficiency of these structures. Then, the paper evaluates the efficiency η for the solar cell with and without Anti-reflection coating ARC on textured surfaces to achieve a final increase of 22.5% of conversion efficiency compared to InGaN standard solar cells.

(Received June 30, 2022; Accepted September 13, 2022)

Keywords: InGaN, Solar cells, Optimization, PC1D

1. Introduction

Over the last couple of decades, Semiconductors of the type III-N are of growing interest through various studies such as gallium nitride (GaN), aluminium nitride (AlN) and indium nitride (InN) with a gap of 3.4eV, 6.2eV and 0.7eV respectively[1–4]. III-N semiconductors has been widely used in optoelectronics, as they have the following characteristics: robust, having a high thermal conductivity, high melting point, and, moreover, a direct forbidden band gap[5]. InGaN possesses the most unique property of direct band ranging from 0.7ev to 3.42 ev which can be adjusted according to the indium composition, therefore it covers approximately the total solar energy spectrum[6,7]. In this study, the solar power conversion efficiency of In0.2Ga0.8N based tandem solar cells was investigated. With this intention, the effects of the most important parameters such as emitter thickness, base thickness, emitter dopant density, base dopant and antireflection coating on the performance of solar cells were studied[8,9]. PC1D software has been chosen as a simulation tool for this research regarding its advantages, simplicity and its user-friendly system [10–12].

In this present work, undoped and Nickel doped zinc oxide (ZnO) thin films have been prepared on glass substrates by spin coating technique. We have investigated the influence of doping concentrations ranging from 0 to 6 at.-% on structural, morphological and optical properties of ZnO thin films[13].

2. Properties of igan used in the simulation

J. Wu et al [7]. and T. Kuykendall [14] et al given the fact that the band-gap energy of the $In_xGa_{1-x}N$ alloys is tunable between 0.7 and 3.4 eV covering the full solar spectrum from the near-

* Corresponding author: houcine.naim@univ-relizane.dz
https://doi.org/10.15251/CL.2022.199.611

ultraviolet to the near-infrared region. $In_xGa_{1-x}N$ ternary alloys present a great potential for applications in solid-state lighting and photovoltaics[14], motivating further development of these materials.

The alloy used in this work consists of $In_{0.2}Ga_{0.8}N$, which has a band gap of 2.642 eV. The cell is chosen to have an area of 1 mm^2. The device is a homo-junction structure whose block diagram is shown in figure 1[15]. It consists mainly of an n-type emitting layer, a P-type base. The model parameters used are described in Table 1.

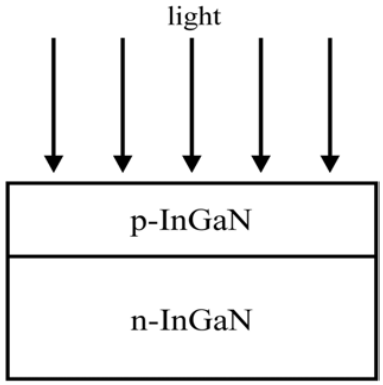

Fig. 1. Structure of an InGaN solar cell.

Undoped and Ni doped zinc oxide thin films deposited by sol-gel spin coating method onto glass substrates.

Table 1. Parameters used in the simulation of the $In_{0.2}Ga_{0.8}N$ reference cell [16,17].

Band Gap (eV)	2.642
Electron Affinity (eV)	4.672
Nc/Nv Ratio	0.03486388
Dielectric Constant	10.18
Electron Mobility (cm^2/Vs)	400
Hole Mobility (cm^2/Vs)	10
Bulk Recombination: tau-n (μs)	10
Bulk Recombination: tau-P (μs)	10
Refractive Index	2.412

In this work, calculations were all performed under ideal conditions (under 1-sun AM1.5 illumination and a temperature of 300 K using the one diode ideal model), and for convenience, several simplifying assumptions were made, including no reflection losses, no series resistance losses, and contact shadowing [8,18,19].

When a PN junction is illuminated with light (as in a solar cell), the generated current creates a forward bias across the PN junction.

$$I = I_L - I_D \tag{1}$$

where
I_L is the light generated current due to the photovoltaic effect.
I_D is the diode current given by Shockley equation.

$$I_D = Is(\exp\frac{V_D}{nV_t} - 1) \tag{2}$$

The total output current drawn from single cells under illumination is given by as:

$$I = I_L - Is(\exp\frac{V_D}{nV_t} - 1) \tag{3}$$

The cell conversion efficiency η of the solar cell expressed as a percentage. It is defined as the ratio between the maximum power (Pmax) delivered by the cell and the incident light power (P0).

$$\eta = \frac{\mathrm{I_m}.V_m}{P_0} \tag{4}$$

The fill factor is defined by:

$$FF = \frac{\mathrm{I_m}.V_m}{I_{sc}.V_{oc}} \tag{5}$$

where
VT is the thermal voltage,
VD is the voltage across the diode,
I is the diode current,
IS is the reverse bias saturation current,
n is the ideality factor,
Im and Vm are coordinates of the maximum power point,
P0 is the total incident solar power.

3. Modeling and simulation

One of the main factors in determining the feasibility of fabricating a photoelectric device is the cost of semiconductor materials. Thus, whatever the structure of the solar cell, improving its parameters is necessary to obtain good efficiency and minimize associated losses such as recombination losses, chain resistance losses, thermal losses, metal / semiconductor contact losses, and reflection losses).

Careful selection of materials with ideal thickness and the doping levels is an important factor in reducing costs while maximizing device efficiency.

3.1. Influence of base parameters on cell performance

We suggested calculating of the base parameters first because it is the weakly doped regions compared to the other regions, In this context, we fixed the parameters of the emitter ($1x10^{18}cm^{-3}$, 0.1µm)and we calculated the characteristic values of the cell according to the thickness and the doping of the base.

By introducing the simulation parameters into the PC1D software and by varying the thickness and the doping. The intervals correspond to the base parameters as follows:

- Base thickness X_B = [50 -400] µm
- Doping of the base $N_A = [1.10^{16} – 5.10^{18}]cm^{-3}$

After this procedure, we got the following results:

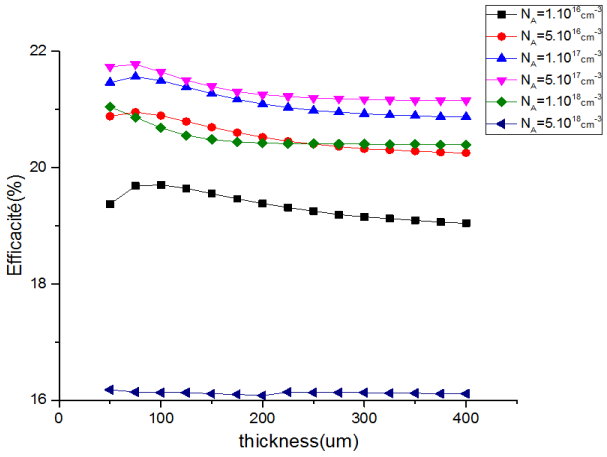

Fig. 2. Effects of doping concentration and thickness layers on the efficiency.

Figure 2 shows the influence of the base parameters (thickness and doping) on the efficiency of the photovoltaic cell. It is noted that the efficiency obtained for a thickness of 75µm and a doping of 5.10^{17} cm^{-3} is 21.76%.

3.2. Influence of the emitter parameters on the Cell performance

After optimizing the base parameters that provide the best conversion efficiency for the PV cells, we try to improve the emitter parameters. To do this study we will set the parameters of the optimal base (75µm, 5.10^{17} cm^{-3}), and vary that of the emitter as follows:

- Emitter thickness X_E = [0.1 -50] µm
- Doping of the emitter N_D = [1.10^{17} – 5.10^{19}] cm^{-3}

After this procedure, we got the following results as shows in figure3:

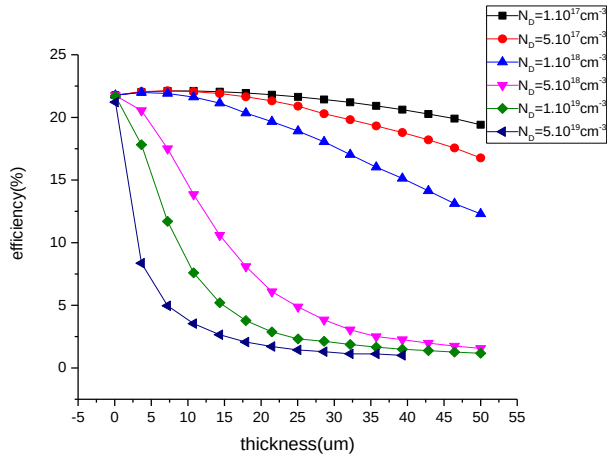

Fig. 3. Effects of doping concentration and thickness layers on the efficiency.

We note that the efficiency takes its optimal value for doping the Emitter with N_D = $5.10^{17}cm^{-3}$ and a thickness of X_E = 7µm.

3.3. Standard solar cell optimized

Studying the influence of different parameters allowed us to optimize the physical and geometric parameters of the solar cell. The optimal values used in the calculation of this work are grouped in the following table2:

Table 2. Values of the optimal parameters.

Base thickness	75µm
Doping of the base	$5.10^{17}cm^{-3}$
Emitter thickness	7µm
Doping of the emitter	$5.10^{17}cm^{-3}$

The current-voltage characteristic of the InGaN solar cell for the optimized values of the cell is shown in Figure4. The simulation results exhibited the highest values of Isc=0.0369A, Voc= 0.7060V, Pmax=0.0221W and maximum efficiency (η) = 22.1%.

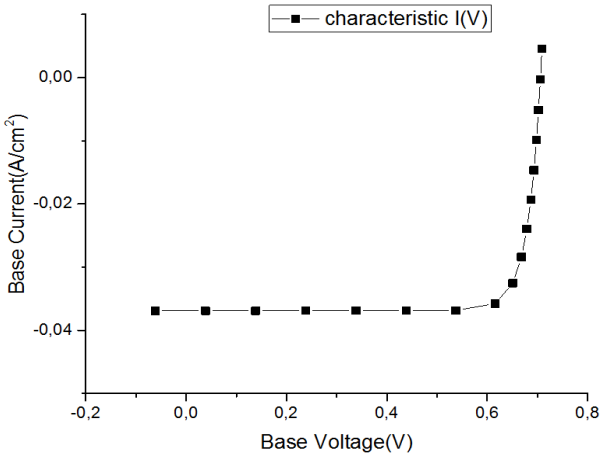

Fig. 4. I-V curve of Standard solar cell optimized.

3.4. Texturing impact on the solar cell

Once the challenges in InGaN material and device design are identified and optimized independently, the next step is to develop InGaN solar cells by comprehensively optimize them.

Texturization on the solar cell is done to reduce reflection and enhance light absorption. Texturization normally creates an uneven surface. that is pyramid-like structures with height 3 µm and having an equal angle of 54.74°[20,21].

The light-trapping mechanism of pyramidal structures is depicted in Fig. 5. The incident light is trapped within the pyramid walls. These pyramidal structures can increase the area of the ZnO/Si hetero junction, resulting in more electron-hole pairs on the p-n junction of solar cells when illuminated. It enhances the efficiency of solar cells based on micro-pyramidal structures.

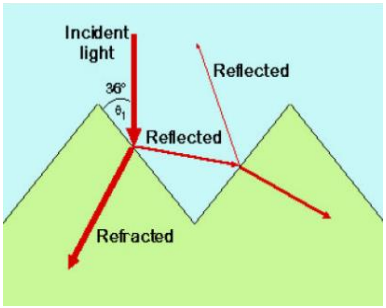

Fig. 5. Light capturing mechanism diagram in silicon surface micro-pyramidal structure.

The performance parameters of the PC1D simulation cells for textured indicate that there is an efficiency gain ranging from 22.1% up to 22.3%.

3.5. Impact of Anti-reflection Coating

Antireflection coating ARC presents thin film of a transparency material with refractive index (n) between those of air (no=1) and (n InGaN = 2.412). ARC reduces the Fresnel reflection caused from light penetration from a medium of one refractive index to another (for example air/semiconductor). The main benefit of using ARC is getting to know the amount of relative improvement that we expect in the performance of solar cells[21].

Different types of single layer ARC (SiO_2, ZnO, TiO_2, SnO_2) are used for reduction for reflectance of InGaN solar cells.

Figure 5 shows reflection from a InGaN wafer having single layer ARC (SiO_2, ZnO, TiO_2, SnO_2), Clear reduction in reflectance for the combination of SnO2 can be seen for broad wavelength range from 530 to 860 nm.

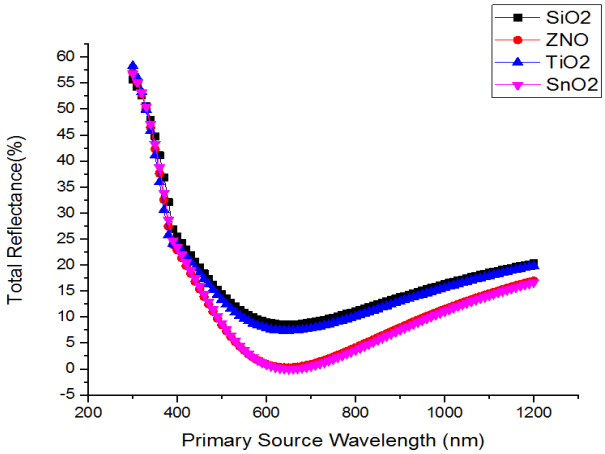

Fig. 6. Anti-reflection Coatings with Different types of single layer.

3.6. Spectral response of a solar cell

The spectral response RS of a photovoltaic cell is the ratio between the short-circuit current generated by the cell and the incident light power. The spectral response RS is given by the following relation[8,22].

$$RS = \frac{I_{sc}(\lambda)}{P_0} \tag{6}$$

The external EQE quantum efficiency of the cell is the ratio of the number of carriers generated on the number of incident photons for each wavelength, it is linked to the spectral response by

$$EQE(\lambda) = RS(\lambda)\frac{h.c}{\lambda.q} \tag{7}$$

External quantum efficiency (EQE) of a solar cell provides information on the internal operations of the solar cells which can be used in optimization of solar cell design.

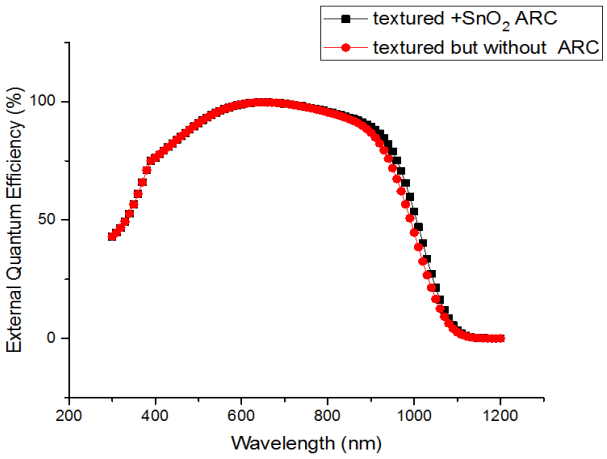

Fig. 7. Simulated EQE characteristics of solar cell device.

The figure shows EQE with and without ARC coating on textured surface, we note that efficiency is low in the area of UV and near IR. its value increases and approaches the value of 99% in the visible domain

4. Results and discussion

The figure 7 shows the comparison of I(V) characteristic of the InGaN between Standard solar cell optimized and with and without ARC coating on textured surface.

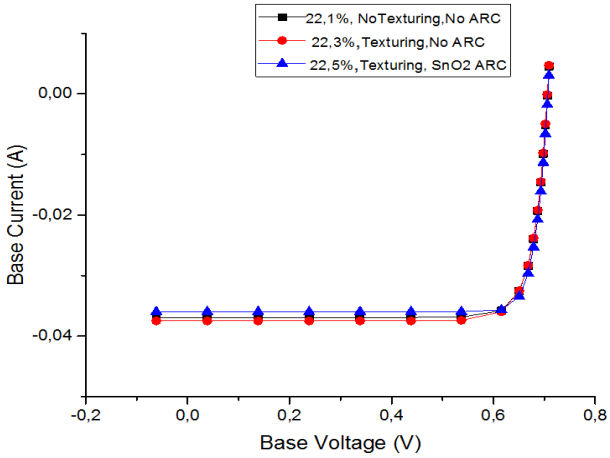

Fig. 8. Comparison of I(V) characteristic of the InGaN.

Table 3. The results of simulation are summarized in the table below.

	Short circuit current (Isc)	Open circuit voltage (Voc)	Efficiency (ŋ)
Standard solar cell optimized	0.0369 (A)	0.7060 (V)	22.1 %
Standard solar cell Textured	0.0375(A)	0.7025 (V)	22.3 %
Standard solar cell Textured + SnO_2 ARC	0.0359(A)	0.7367 (V)	22.5 %

From the results of table3, it is seen that the efficiency improves to 21.1 % and 22.5 % for adding of Textured+SnO_2 ARC to InGaN standard solar cell respectively.

5. Conclusion

In this contribution, we have shown how to optimize solar cell parameters used in the simulation by PC1D software.

We have demonstrated that the best magnitudes for emitter thickness, base thickness, emitter dopant density and base dopant densities are 7 µm, 75 µm, $5.10^{17}cm^{-3}$ and $5 \times 10^{17}cm^{-3}$ respectively, in order to obtain 22.1% efficiency InGaN standard solar cells.

It is seen that the textured surface and an anti-reflection coating reduces reflection and increases the efficiency of the solar cell by up to 22.5%.

References

[1] H. Helal, Z. Benamara, A.H. Kacha, M. Amrani, A. Rabehi, B. Akkal, G. Monier, C. Robert-Goumet, Superlattices Microstruct. 135 (2019) 106276; https://doi.org/10.1016/j.spmi.2019.106276

[2] A. Khettou, I. Zeydi, M. Chellali, M. Ben Arbia, S. Mansouri, H. Helal, H. Maaref, Superlattices Microstruct. 142 (2020) 106539; https://doi.org/10.1016/j.spmi.2020.106539

[3] S. Haghkish, A. Asgari, (n.d.) 1-8.

[4] T. Matsuoka, H. Okamoto, M. Nakao, H. Harima, E. Kurimoto, Appl. Phys. Lett. 81 (2002) 1246-1248; https://doi.org/10.1063/1.1499753

[5] X. Cai, X. Zhou, Z. Liu, F. Jiang, Q. Yu, Optik (Stuttg). 164 (2018) 105-113; https://doi.org/10.1016/j.ijleo.2018.02.102

[6] W. Yang, H. Yu, J. Tang, Y. Su, Q. Wan, Y. Wang, Sol. Energy 85 (2011) 2551-2559; https://doi.org/10.1016/j.solener.2011.07.015

[7] J. Wu, W. Walukiewicz, K.M. Yu, W. Shan, J.W. Ager, E.E. Haller, H. Lu, W.J. Schaff, W.K. Metzger, S. Kurtz, J. Appl. Phys. 94 (2003) 6477-6482; https://doi.org/10.1063/1.1618353

[8] S. Ben Bouzid, F; Machiche, Rev. Des Energies Renouvelables 14 (2011) 47-56.

[9] C. Boudaoud, A. Hamdoune, Z. Allam, Math. Comput. Simul. 167 (2020) 194-201; https://doi.org/10.1016/j.matcom.2018.09.007

[10] L.A. Vilbois, A. Cheknane, A. Bensaoula, C. Boney, T. Benouaz, Energy Procedia 18 (2012) 795-806; https://doi.org/10.1016/j.egypro.2012.05.095

[11] A. Üzüm, A. Mandong, 23 (2019) 1190-1197; https://doi.org/10.16984/saufenbilder.557490

[12] C.S. Solanki, B.M. Arora, J. Vasi, M.B. Patil, C.S. Solanki, B.M. Arora, J. Vasi, M.B. Patil, Sol. Photovoltaics (2013) 130-146; https://doi.org/10.1017/9789382993254

[13] H. Naim, D.K. Shah, A. Bouadi, M.R. Siddiqui, M.S. Akhtar, C.Y. Kim, J. Electron. Mater. 51 (2022) 586-593; https://doi.org/10.1007/s11664-021-09341-5

[14] T. Kuykendall, P. Ulrich, S. Aloni, P. Yang, Nat. Mater. 6 (2007) 951-956; https://doi.org/10.1038/nmat2037

[15] A. Dussaigne, F. Barbier, B. Samuel, A. Even, R. Templier, F. Lévy, O. Ledoux, M. Rozhavskaia, D. Sotta, J. Cryst. Growth 533 (2020) 125481; https://doi.org/10.1016/j.jcrysgro.2020.125481

[16] X. Zhang, X. Wang, H. Xiao, C. Yang, J. Ran, C. Wang, Q. Hou, J. Li, J. Phys. D. Appl. Phys. 40 (2007) 7335-7338; https://doi.org/10.1088/0022-3727/40/23/013

[17] O.K. Jani, I.P. Fulfillment, East (2008) 154; https://doi.org/10.1016/j.gie.2007.07.013

[18] M. Mehta, (2008) 3-7.

[19] B. Chouchen, A. El, M. Hichem, A. Bajahzar, Opt. - Int. J. Light Electron Opt. 199 (2019) 163385; https://doi.org/10.1016/j.ijleo.2019.163385

[20] T. Dzhafarov, Sol. Cells - Res. Appl. Perspect. (2013).
[21] C.S. Solanki, H.K. Singh, (2017).
[22] H. Mäckel, A. Cuevas, (2014).